
Mass Dependency of the Dressed Polyakov Loop in the NJL Model

Massenabhängigkeit des gedressten Polyakovloops im NJL Modell

Bachelor-Thesis von Stephan Wezorke

26. September 2012



TECHNISCHE
UNIVERSITÄT
DARMSTADT

Fachbereich Physik
Institut für Kernphysik
NHQ group

Mass Dependency of the Dressed Polyakov Loop in the NJL Model
Massenabhängigkeit des gedressten Polyakovloops im NJL Modell

Vorgelegte Bachelor-Thesis von Stephan Wezorke

1. Gutachten: Priv. Doz. Dr. Michael Buballa
2. Gutachten: Prof. Dr. Jochen Wambach

Tag der Einreichung:

Selbstständigkeitserklärung

Hiermit erkläre ich, dass ich die vorliegende Bachelorarbeit selbstständig und nur unter Verwendung der angegebenen Literatur und Hilfsmittel angefertigt habe. Die aus fremden Quellen direkt oder indirekt übernommenen Stellen sind als solche kenntlich gemacht.

Die Arbeit wurde bisher in gleicher oder ähnlicher Form keiner anderen Prüfungsbehörde vorgelegt und auch nicht veröffentlicht.

Darmstadt, den 9. Juli 2012

(Stephan Wezorke)

Abstract

The chiral quark condensate and the dressed Polyakov loop are investigated in a two-flavor NJL model in the mean field approximation. In quantum chromodynamics the chiral quark condensate is an exact order parameter for chiral symmetry breaking in the chiral limit, whereas the dressed Polyakov loop is an order parameter for confinement for infinite bare quark masses. For this reason, both quantities are particularly examined at vanishing and high bare quark mass and it is checked, whether the expectations derived from quantum chromodynamics are fulfilled. We furthermore derive the T - μ -phase diagram from both quantities.

Zusammenfassung

Das chirale Quarkkondensat und der gedresste Polyakov-Loop werden in einem NJL Modell mit zwei Quarkflavors in Mean-Field-Näherung untersucht. In der Quantenchromodynamik ist das chirale Quarkkondensat ein exakter Ordnungsparameter im chiralen Limes, wohingegen der „dressed“ Polyakov-Loop ein Ordnungsparameter für Confinement bei unendlicher nackter Quarkmasse ist. Aus diesem Grund werden beide Größen insbesondere bei verschwindender und großer nackter Quarkmasse untersucht und es wird überprüft, ob die Erwartungen aus der Quantenchromodynamik erfüllt sind. Darüberhinaus werden die T - μ -Phasendiagramme zu beiden Größen ermittelt.

Contents

1. Introduction	4
2. Theoretical Basics	6
2.1. The Nambu–Jona-Lasinio-Model	6
2.1.1. Effective Mass	6
2.1.2. NJL Model at Finite Temperature and Quark Chemical Potential	8
2.1.3. Model Parameters	10
2.2. Arbitrary Boundary Condition	10
2.2.1. The Dressed Polyakov Loop	11
3. Numerical Results	13
3.1. Fermionic Chiral Condensate	13
3.2. Bosonic Chiral Condensate	13
3.3. ϕ -dependent Chiral Condensate	15
3.4. Chiral Condensate without Thermal Cutoff	17
3.5. Consequences on the Dressed Polyakov Loop	19
3.6. The Dressed Polyakov Loop as an Order Parameter	19
3.7. Conclusion	23
4. Summary and Outlook	24
A. Motivation for the Matsubara Replacement in Thermal Field Theory	25

1 Introduction

Quantum chromodynamics (QCD) is the physical theory that describes interaction of quarks and gluons, which are part of the set of elementary particles described by the standard model of particle physics. Quarks are particles that obey the strong interaction which is a force acting on the color charge of a particle and is transmitted by its gauge bosons, the gluons. Due to the fact, that the force between two quarks does not decrease with their distance, one cannot observe single quarks in nature; they always stick together as hadrons, which is called confinement.

Two famous, unsolved problems that researchers focus on nowadays are the analytical proof of confinement in QCD and the localization of phase transitions in the QCD T - μ -phase diagram. Understanding the last one shall help to explain the creation of hadronic matter in the early universe. A forthcoming project from which one expects to shed light on the QCD phase diagram is the new accelerator “FAIR”, being built at “GSI Helmholtzzentrum für Schwerionenforschung” in Darmstadt the next years.

Since gluons themselves underly the strong interaction, which makes it almost impossible to do any exact calculations, theoretical approaches to deal with the above-named problems are rather complex. Even though it is possible to calculate cross sections perturbatively and therefore gain information about interactions occurring in quantum chromodynamics, the computation of many-body interactions is barely possible. This is why the thermodynamic behavior of quarks and gluons is hardly understood.

A possible workaround is using effective models, that share symmetry properties with the QCD and hence facilitate the exact calculation of observables in QCD alike quantum field theories. The attempt is to gain information using effective theories, which help to understand the behavior of quarks and gluons in QCD. The Nambu–Jona-Lasinio model is one convenient model, that can be used to explore quarks and their properties. Although the NJL model does not include any confinement, it is possible to calculate observables that are or might be order parameters for the confined phase in other models, which opens up the opportunity to check which observables might serve as an order parameter for confinement, and which do not.

Two important quantities in QCD are the chiral quark condensate (or chiral condensate), that is an exact order parameter for chiral symmetry in the chiral limit, $m = 0\text{MeV}$, and the Polyakov loop, which is an order parameter for confinement in case of infinite bare quark masses, $m = \infty$. Lattice calculations have shown that in the range of realistic quark masses both parameters indicate a cross-over transition. According to these calculations the two cross-overs occur at approximately the same temperature. Another quantity is the dressed Polyakov loop, that equals the Polyakov loop in the limit $m = \infty$, hence the dressed Polyakov loop is an order parameter for confinement, too.

The NJL model includes chiral symmetry and the chiral quark condensate can be easily calculated, but the model does not include any gluons, thus the Polyakov loop can not be defined. However, it is possible to compute the dressed Polyakov loop.

In QCD one expects the chiral cross-over to become sharper in the chiral limit, since the cross-over passes into a phase transition, and blurred at large bare quark masses. On the contrary the cross-over implied by the dressed Polyakov loop should become sharper with increasing bare

quark masses.

In this work the behavior of the dressed Polyakov loop and chiral condensate is investigated in the chiral limit and at large bare quark masses, to check, whether the expectations of quantum chromodynamics are fulfilled in the NJL model.

2 Theoretical Basics

2.1 The Nambu–Jona-Lasinio-Model

The Nambu–Jona-Lasinio model had been introduced by Y. Nambu and G. Jona-Lasinio in [1] in 1961 and extended in [2] in the same year. It was an approach to explain the mass of nucleons, before the idea of quarks has been developed. Nambu and Jona-Lasinio suggested, that the nucleon mass arises as the self-energy of self-interacting fermions. These fermions were supposed to obey an attractive force between particle and antiparticle in order to form a fermion condensate.

Since quarks have been discovered to be the real components of nucleons, the original interpretation of the NJL model is outdated. Nevertheless, it is used as an effective model of quarks, nowadays. The Lagrangian is given by

$$\mathcal{L} = \bar{\psi} (i\rlap{/}{\partial} - m) \psi + G \left[(\bar{\psi}\psi)^2 + (\bar{\psi}i\gamma_5\tau_a\psi)^2 \right], \quad (2.1)$$

where τ_a denotes the Pauli matrices in isospin space and m the bare quark mass. The two-flavor NJL model describes an up and a down quark, therefore the mass m is a matrix given by $\text{diag}(m_{up}, m_{down})$. Due to the fact, that the quark masses of the up and down quark are hardly dissimilar (compared to the much heavier nucleons), one uses the simplification of identical masses $m = m_u = m_d$.¹

In case of $m = 0$ MeV, the Lagrangian splits up into two independent parts, a right-handed and a left-handed one, describing a right-handed and left-handed field ψ_r and ψ_l , respectively. Both parts of the Lagrangian have their own $SU(2)$ symmetry with the symmetry transformation

$$\psi \rightarrow e^{-i\vec{\theta}\vec{\tau}}\psi, \quad (2.2)$$

such that the full Lagrange density is invariant under a global $SU(2)_r \times SU(2)_l$ symmetry, which is also called chiral symmetry. $\vec{\tau}$ denotes the vector of Pauli matrices, the generators of $SU(2)$.

Besides the chiral symmetry (if $m = 0$ MeV), the Lagrangian is invariant under a global $U(1)$ transformation ($\psi \rightarrow e^{-ia}\psi$, $a \in \mathbb{R}$). According to this, the NJL model has the same global symmetry as the Lagrangian of quantum chromodynamics and is assumed to have analog effects.

2.1.1 Effective Mass

The effective mass, that was supposed to explain the nucleon mass, arises due to self-interaction occurring in all quantum field theories. The diagrammatic self-interaction is shown in figure 2.1. Translating this diagram in an equation yields

$$iS_d(p) = iS_b(p) + iS_b(p)(-i\Sigma)iS_b(p) + \dots = iS_b(p) + iS_b(p)\Sigma S_d(p), \quad (2.3)$$

¹ Actually, the mass matrix reads $\text{diag}(m, m) = m\mathbb{I}$, but multiplications with \mathbb{I} are usually omitted and will not be explicitly written down in this work.

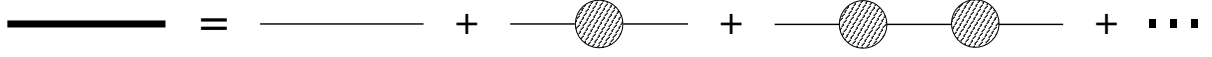


Figure 2.1.: Diagrammatic illustration of the self-interaction. The bold and thin line stand for the dressed and bare quark propagator, respectively. The circles are one-particle irreducible diagrams, constituting the self-energy.

where Σ describes the self-energy and

$$S_d(p) = \frac{\not{p} + M}{p^2 - M^2 + i\epsilon} \quad (2.4)$$

and

$$S_b(p) = \frac{\not{p} + m}{p^2 - m^2 + i\epsilon} \quad (2.5)$$

denote the dressed and bare fermion propagator, respectively. Multiplying equation (2.3) with the inverse propagators $S_d^{-1}(p) = \not{p} - M + i\epsilon$ and $S_b^{-1}(p) = \not{p} - m + i\epsilon$ yields the relation between bare and effective quark mass:

$$M = m + \Sigma \quad (2.6)$$

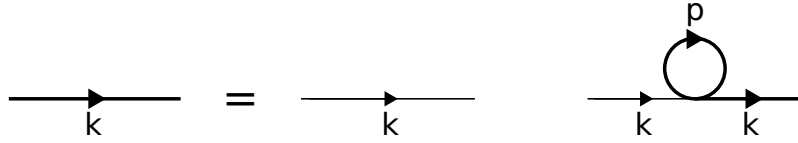


Figure 2.2.: Simple Feynman diagram of the dressed propagator.

The self-energy Σ can be determined applying Feynman rules to figure 2.2:

$$\Sigma = 2G \int \frac{d^4p}{(2\pi)^4} Tr \{iS_d(p)\} + 2G \cdot i\gamma_5 \tau_a i \int \frac{d^4p}{(2\pi)^4} Tr \{i\gamma_5 \tau_a S_d(p)\}, \quad (2.7)$$

where the trace is performed in Dirac, color and flavor space. Taking into account that the trace of an odd number of gamma matrices vanishes and $Tr \mathbb{1} = 4N_f N_c$ (4-dimensional Dirac space and degeneracy in flavor and color space), the self-energy can be written as

$$\Sigma = 8GN_f N_c \int \frac{d^4p}{(2\pi)^4} \frac{iM}{p^2 - M^2 + i\epsilon} \quad (2.8)$$

Using the residual theorem and the residue $R = -\frac{1}{2E_p}$ in $p_0 = -\sqrt{E_p^2 + i\epsilon}$ with $E_p = \sqrt{\vec{p}^2 + M^2}$, one can perform the time-integration $\int_{-\infty}^{\infty} \frac{dp_0}{2\pi}$ in equation (2.8):

$$\Sigma = 8iGMN_f N_c \int \frac{d^3p}{(2\pi)^4} \frac{2\pi i}{-2E_p} = 4GMN_f N_c \int \frac{d^3p}{(2\pi)^3} \frac{1}{E_p} \quad (2.9)$$

Transforming this integral to spherical coordinates, the angular integration can be performed. All in all one obtains the following equation that can be solved numerically in order to estimate the effective mass M :

$$M = m + \frac{2N_f N_c}{\pi^2} GM \cdot \int_0^\Lambda dp \frac{p^2}{E_p} \quad (2.10)$$

Since the integral is divergent, a momentum cutoff is applied as regularization. For a finite cutoff parameter Λ , the above integral can be solved analytically and equation (2.10) reads

$$M = m + \frac{2N_f N_c}{\pi^2} GM \cdot \left(-\frac{1}{2} M^2 \cdot \operatorname{asinh} \left(\frac{\Lambda}{|M|} \right) + \frac{1}{2} \Lambda \sqrt{\Lambda^2 + M^2} \right) \quad (2.11)$$

2.1.2 NJL Model at Finite Temperature and Quark Chemical Potential

In order to analyze the T - μ -phase diagram mentioned above, it is not sufficient to calculate quantities at zero temperature and quark chemical potential. Calculating physical observables at finite temperature and chemical potential, one has to consider a thermal field theory formalism. One of these formalisms is the Matsubara formalism (also referred to as imaginary time formalism), in which the time integral is replaced by a discrete sum over so called Matsubara frequencies ω_n :

$$\int \frac{dp_0}{2\pi} f(p_0, \vec{p}) \longrightarrow iT \sum_{n=-\infty}^{\infty} f(i\omega_n + \mu, \vec{p}) \quad (2.12)$$

A brief motivation for this transition is given in appendix A based on [3] and [4], where more detailed introductions to thermal field theory can be found. One important result is, that fermionic and bosonic fields are liable to the boundary conditions

$$\phi(\vec{x}, 0) = \pm \phi(\vec{x}, \beta), \quad (2.13)$$

where the \pm -sign indicates the different boundary conditions for bosons (+) and fermions (-).

Given the mode expansion

$$\phi(\vec{x}, t) = \sum_{n \in \mathbb{N}} e^{i\omega_n t} \phi_n(\vec{x}), \quad (2.14)$$

one can use the periodicity (2.13) to calculate the Matsubara frequencies:

$$\phi(\vec{x}, 0) = \pm \phi(\vec{x}, \beta) \quad (2.15)$$

$$\Leftrightarrow \sum_{n \in \mathbb{N}} \phi_n(\vec{x}) = \pm \sum_{n \in \mathbb{N}} e^{i\omega_n \beta} \phi_n(\vec{x}) \quad (2.16)$$

Equation (2.16) yields the bosonic and fermionic Matsubara frequencies, respectively:

$$\omega_n^{(b)} = 2n\pi T \quad (2.17)$$

$$\omega_n^{(f)} = (2n + 1)\pi T \quad (2.18)$$

Using the replacement (2.12), the effective mass at finite temperature and quark density can be written as

$$M = m - 8GMN_f N_c \int \frac{d^3p}{(2\pi)^3} \sum_{n \in \mathbb{Z}} \frac{T}{(i\omega_n + \mu)^2 - E_p^2} \quad (2.19)$$

A convenient method to solve this equation is using the residue theorem backwards to replace the Matsubara sum by an integral in the complex plane (see [5] for an explicit calculation). Afterwards, the path of this integral can be changed to surround both poles near the real axis. In a last step, the integral can be replaced using the residue theorem to obtain the following formula:

$$M = m - 2GM \frac{N_c N_f}{\pi^2} \left\{ \int_0^\Lambda dp \frac{p^2}{E_p} - \int_0^\Lambda dp \frac{p^2}{E_p} \left[\frac{1}{1 + e^{-\beta(E_p - \mu)}} + \frac{1}{1 + e^{-\beta(E_p + \mu)}} \right] \right\} \quad (2.20)$$

The effective mass is closely related to the vacuum expectation value $\langle \bar{\psi}\psi \rangle$ of $\bar{\psi}\psi$, which is the so called chiral or quark condensate and is in general defined as

$$\langle \bar{\psi}\psi \rangle = -i \int \frac{d^4p}{(2\pi)^4} \text{Tr} \{S(p)\}. \quad (2.21)$$

Comparing this definition with equation (2.7) immediately yields the relation

$$\langle \bar{\psi}\psi \rangle = -\frac{\Sigma}{2G} = \frac{m - M}{2G}. \quad (2.22)$$

In the chiral limit, the chiral condensate is an exact order parameter for chirality, since it is proportional to the effective mass if $m = 0$ MeV. Chiral symmetry is spontaneously broken if $M > 0$ MeV, which means, that the effective mass equals zero, when the chiral symmetry is restored.

The expectation value of the pseudo-scalar interaction channel vanishes, since a similar definition like in equation (2.21) is zero due to $\text{Tr} \{i\gamma_5 \tau_a S(p)\} = 0$. The trace vanishes since the trace over the pauli matrices equals zero.

The solution of equation (2.24) is not necessarily unique, so that one has to consider, which solution is the correct one. In statistical physics the a stable solution is specified by the global minimum of a thermodynamic potential. Since temperature and chemical potential are fixed, the grand canonical potential is suitable for estimating the physically relevant solution.

In order to derive the grand canonical potential in mean field approximation one has to linearize the Lagrangian using the vacuum expectation value $\langle \bar{\psi}\psi \rangle$.

Using the relation (2.22), the Lagrangian can be written in mean field approximation (like done in [6]) as

$$\mathcal{L} = \bar{\psi}(i\rlap{\not{d}} - M)\psi - \frac{(m - M)^2}{4G}, \quad (2.23)$$

which describes non-interacting quasi particles of mass M in a constant, global potential. That means, that the grand potential is a sum of the mass term and a free quark gas contribution (see [6] for a more detailed derivation):

$$\Omega = \frac{(m - M)^2}{4G} - \frac{N_c N_f}{\pi^2} \left\{ \int_0^\Lambda dp p^2 E_p + \int_0^\Lambda dp p^2 T \left[\ln(1 + e^{-\beta(E_p - \mu)}) + \ln(1 + e^{-\beta(E_p + \mu)}) \right] \right\} \quad (2.24)$$

One can show, that the self-consistency equation (2.20) is equivalent to $\frac{\partial \Omega}{\partial M} = 0$.

2.1.3 Model Parameters

The model parameters are chosen as $\Lambda = 631.5$ MeV, $G \cdot \Lambda^2 = 2.193$ and $m = 5.5$ MeV, taken from [7]. In order to investigate the behavior of the dressed Polyakov loop (see section 2.2.1) as an order parameter, various bare quark masses are used throughout this work. Therefore the bare mass parameter $m = 5.5$ MeV will be referred to as conventional bare quark mass.

The thermal part of the integral in equation (2.20) and (2.24) is not divergent and thus does not need to be regularized. Nevertheless, the cutoff is applied to this part of the integral in this work.

2.2 Arbitrary Boundary Condition

The boundary conditions that have been introduced in equation (2.13) arise due to the definition of the time-ordered product for bosons and fermions (see appendix A). Nevertheless, these boundary conditions can be generalized to

$$\psi(\vec{x}, x^0) = e^{i\phi} \psi(\vec{x}, x^0 + \beta), \quad (2.25)$$

with an arbitrary phase parameter $\phi \in [0, 2\pi]$. Using the mode expansion (2.14) as done before, one can calculate Matsubara frequencies depending on the arbitrary phase parameter ϕ :

$$\psi(\vec{x}, 0) = e^{i\phi} \psi(\vec{x}, \beta) \quad (2.26)$$

$$\Leftrightarrow \sum_{n \in \mathbb{N}} \psi_n(\vec{x}) = e^{i\phi} \sum_{n \in \mathbb{N}} e^{i\omega_n \beta} \psi_n(\vec{x}) = \sum_{n \in \mathbb{N}} e^{i(\omega_n \beta + \phi)} \psi_n(\vec{x}) \quad (2.27)$$

$$\Leftrightarrow 2\pi n = \omega_n \beta + \phi \quad (2.28)$$

According to equation (2.28), the Matsubara frequencies for arbitrary boundary conditions read

$$\omega_n = (2\pi n - \phi)T. \quad (2.29)$$

The two special cases of bosonic and fermionic Matsubara frequencies emerge when $\phi = 0$ and $\phi = \pi$, respectively. Applying the new Matsubara frequencies to the model yields slightly different equations for the grand canonical potential and effective mass. The easiest way to

evaluate the new expressions is by defining an complex chemical potential $\tilde{\mu}$ as $\tilde{\mu} = \mu - iT(\phi - \pi)$, that encapsulates the phase parameter. Using the replacement $\mu \rightarrow \tilde{\mu}$ one obtains the ϕ -dependent grand potential

$$\Omega_\phi = \frac{(m - M)^2}{4G} - \frac{N_c N_f}{\pi^2} \left\{ \int_0^\Lambda dp p^2 E_p + \int_0^\Lambda dp p^2 T \left[\ln \left(1 + e^{-\beta(E_p - \mu) - iT(\phi - \pi)} \right) + \ln \left(1 + e^{-\beta(E_p + \mu) + iT(\phi - \pi)} \right) \right] \right\}. \quad (2.30)$$

The same replacement can be done to get the ϕ -dependent self-consistency equation of the effective mass. The term $iT(\phi - \pi)$ is only part of the exponent and therefore only occurs in the exponential function of the derivative $\frac{\partial \Omega_\phi}{\partial M}$. This means, in turn, that $\frac{\partial \Omega_\phi}{\partial M} = 0$ is still equivalent to equation (2.20) when replacing μ with $\tilde{\mu}$ and that the ϕ -dependent self-consistency equation of the effective mass can be written as

$$M_\phi = m - 2GM_\phi \frac{N_c N_f}{\pi^2} \left\{ \int_0^\Lambda dp \frac{p^2}{E_p} - \int_0^\Lambda dp \frac{p^2}{E_p} \left[\frac{1}{1 + e^{-\beta(E_p - \mu) - iT(\phi - \pi)}} + \frac{1}{1 + e^{-\beta(E_p + \mu) + iT(\phi - \pi)}} \right] \right\}. \quad (2.31)$$

Since the grand canonical potential and effective mass depend on the phase parameter ϕ , one obtains a ϕ -dependent chiral condensate, too, whose definition is the same as in equation (2.22):

$$\langle \bar{\psi} \psi \rangle_\phi = \frac{m - M_\phi}{2G}. \quad (2.32)$$

Note that the summand π in $\tilde{\mu}$ is arbitrary but chosen this way that we receive the former quantities when ϕ equals π , corresponding to fermionic boundary conditions. Accordingly, $\langle \bar{\psi} \psi \rangle_0$ and $\langle \bar{\psi} \psi \rangle_\pi$ will be referred to as bosonic and fermionic chiral condensate, respectively.

Depending on the choice of ϕ the grand potential might become complex, which means, that the minimum of Ω_ϕ is undefined. Thus only its real component is minimized. Furthermore, the effective mass might be complex, too, so that one can calculate the derivative of Ω_ϕ with respect to the imaginary part of M_ϕ additionally. Since neglecting $\frac{\partial \Omega_\phi}{\partial M_\phi} = 0$ is a common simplification, the ‘‘imaginary’’ derivative is not taken into account; besides, an imaginary mass is unphysical.

2.2.1 The Dressed Polyakov Loop

Using the ϕ -dependent chiral condensate, one can define the so called dressed Polyakov loop as Fourier transformation of $\langle \bar{\psi} \psi \rangle_\phi$ (see [8]):

$$\Sigma^{(1)} = \int_0^{2\pi} \frac{d\phi}{2\pi} e^{-i\phi} \langle \bar{\psi} \psi \rangle_\phi. \quad (2.33)$$

The dressed Polyakov loop is related to the “thin” Polyakov loop (referred to as Polyakov loop), that is a Wilson-loop closed around time direction. In lattice QCD, the origin of the Polyakov loop, it is an exact order parameter for confinement in the limit of infinite bare quark masses. One expects the Polyakov loop and dressed Polyakov loop to be equal in the limit of infinite bare quark masses $m \rightarrow \infty$. The NJL model does not include any gluons, which means, that the Polyakov loop can not be defined in this model.

It is still interesting to check the behavior of the dressed Polyakov loop at large bare quark masses: On the one hand one expects the dressed Polyakov loop to differ from the chiral condensate, which is no order parameter for confinement; but on the other hand, the NJL model lacks gluons, confinement and the thin Polyakov loop, so that the dressed Polyakov loop might still correlate with the chiral condensate for $m \rightarrow \infty$.

It should be mentioned, that the imaginary part of the dressed Polyakov loop vanishes identically (see [9]), which is why only the real part of $\Sigma^{(1)}$ is considered in this work.

3 Numerical Results

3.1 Fermionic Chiral Condensate

Using the grand canonical potential, one can easily calculate the constituent quark mass for arbitrary temperature and quark chemical potential, which, in turn, can be used to calculate the chiral condensate via equation (2.22).

A T - μ -diagram of the fermionic chiral condensate for the conventional bare quark mass is plotted in figure 3.1(a), where the chiral condensate is normalized to its maximum at $T = \mu = 0$ MeV. In the range of small values of $\frac{\mu}{T}$, no phase transition but a cross-over occurs, while the changeover for small values of T is a first-order phase transition. The critical point of this diagram is located in between.

The figures 3.1(b), 3.2(a) and 3.2(b) show the normalized chiral condensate for bare quark masses $m = 0$ MeV, $m = 55$ MeV and $m = 550$ MeV, respectively. In the chiral limit, the first-order phase transition remains, while the crossover turned into a second-order phase transition. In this case the chiral condensate is an exact order parameter and the border, where it drops to zero is the phase border of the chiral phase diagram in the chiral limit.

The diagrams for tenfold and hundredfold bare quark masses possess a first-order phase transition for large values of $\frac{\mu}{T}$ and a crossover apart from that, just as the conventional diagram.

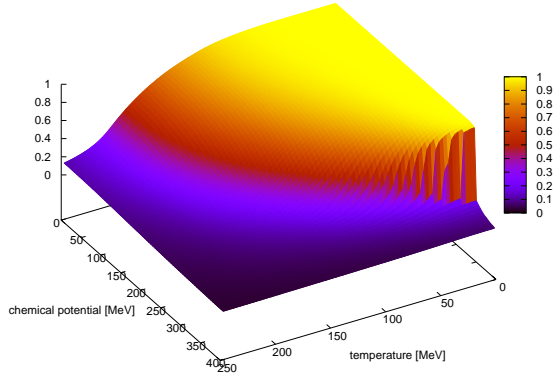
Note that the chiral condensate decreases much more slowly with increasing bare quark mass. Nevertheless, the chiral condensate drops asymptotically to zero for all values of $\frac{\mu}{T}$ with increasing the temperature.

3.2 Bosonic Chiral Condensate

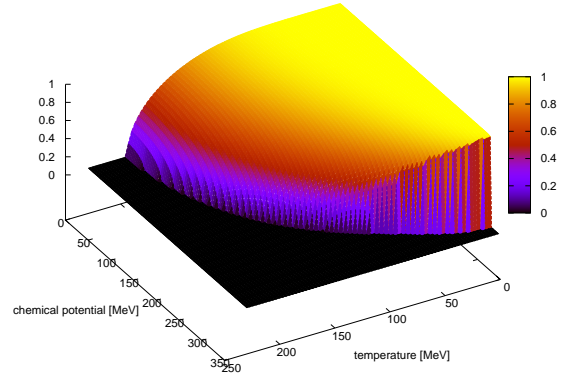
To understand the ϕ -dependent chiral condensate, it is helpful to have a look at the chiral condensate for bosonic boundary condition $\phi = 0$, as plotted in figures 3.3(a) to 3.4(b)¹. One can see that for $\mu = 0$ MeV, the condensate seems to be unbounded or at least monotonously increasing, that is, no phase transition or crossover occurs in this case. This is why the the chiral condensate can not be normalized to its maximal value, like done in the fermionic case. In order to achieve comparability, the bosonic chiral condensate is divided by its value at $T = \mu = 0$ MeV, too, which happens to be identical to the value of the fermionic chiral condensate at $T = \mu = 0$ MeV. On the other hand, the bosonic chiral condensate converges to zero alongside every path $\mu \geq T$. Note that the phase transition is of first order in the bosonic realm independent of the bare quark mass, unlike the cross-over of the fermionic chiral condensate.

One can see, that in the range of $T \gtrsim 400$ MeV the occurring phase transition for $m = 550$ MeV causes the chiral condensate to drop to negative values at first, before it converges to zero. More detailed plots show, that this behavior occurs for every positive bare quark mass.

¹ Please note, that the viewing direction differs from the one in section 3.1 so that the T - and μ -axis seem to be swapped.

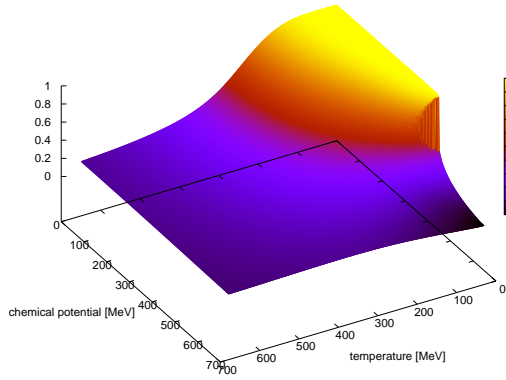


(a) regular bare quark mass, $m = 5.5$ MeV

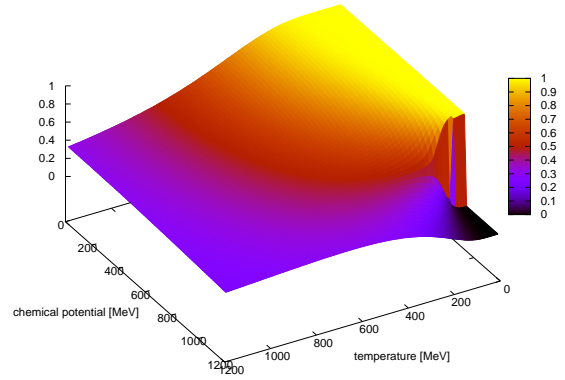


(b) chiral limit, $m = 0$ MeV

Figure 3.1.: Chiral condensate using the conventional parameter set (lhs.) and in the chiral limit (rhs.). Both plots have been normalized to the expectation values at $T = \mu = 0$ MeV.

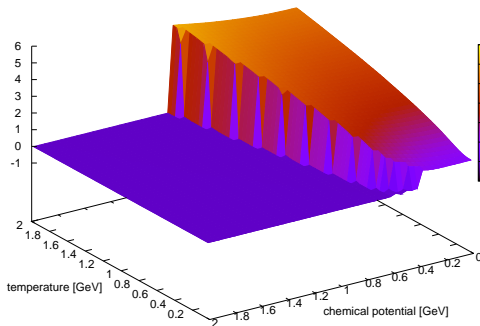


(a) $m = 55$ MeV

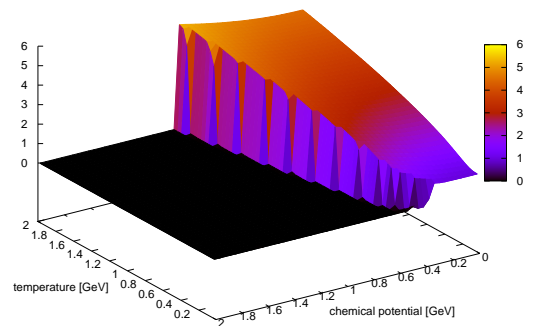


(b) $m = 550$ MeV

Figure 3.2.: Chiral condensate for higher bare quark masses, normalized to its largest values at $T = \mu = 0$ MeV.

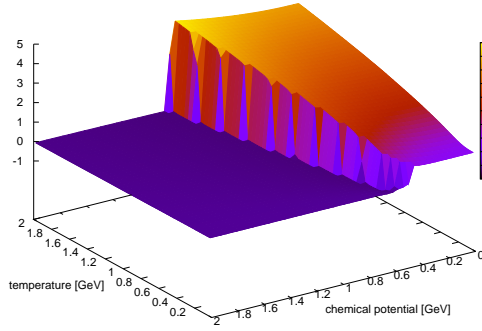


(a) regular bare quark mass, $m = 5.5$ MeV

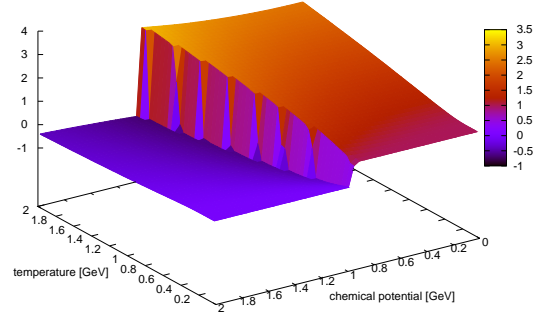


(b) chiral limit, $m = 0$ MeV

Figure 3.3.: Bosonic, chiral condensate using the conventional parameter set (lhs.) and in the chiral limit (rhs.). The same scale factor as used in figures 3.1(a) and 3.1(b) is applied.

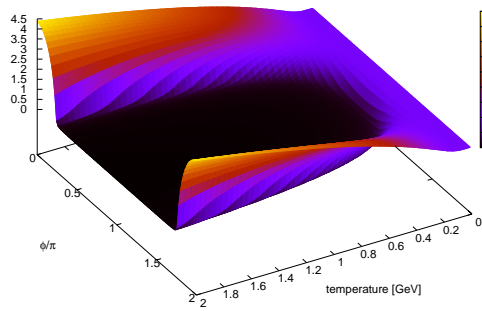


(a) $m = 55 \text{ MeV}$

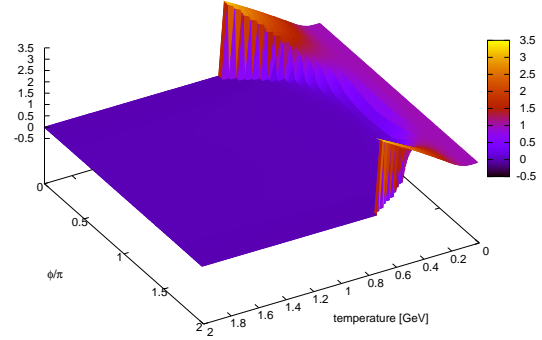


(b) $m = 550 \text{ MeV}$

Figure 3.4.: Bosonic, chiral condensate for higher bare quark masses, normalized to the same values as 3.2(a) and 3.2(b), respectively.



(a) $\mu = 0 \text{ MeV}$



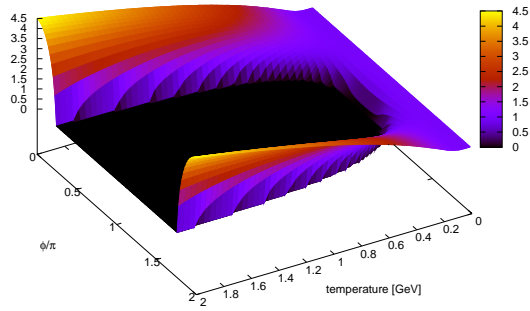
(b) $\mu = T$

Figure 3.5.: ϕ -dependent chiral condensate for $m = 5.5 \text{ MeV}$, normalized to its value at $T = 0 \text{ MeV}$

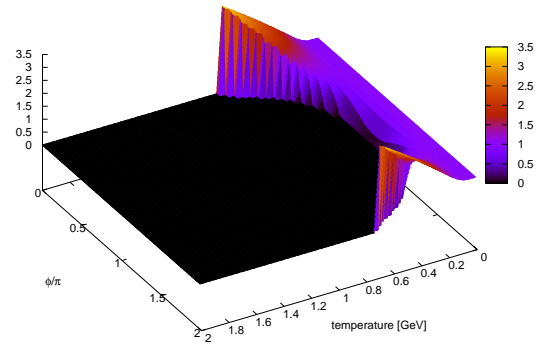
3.3 ϕ -dependent Chiral Condensate

In addition to the two special cases $\langle \bar{\psi}\psi \rangle_{\phi=0}$ and $\langle \bar{\psi}\psi \rangle_{\phi=\pi}$ discussed in the sections above, one needs to analyze the general chiral condensate in order to understand the behavior of the dressed Polyakov loop. The figures 3.5(a) to 3.8(a) show the ϕ -dependent chiral condensate over the temperature and boundary condition ϕ . For each mass parameter used before, two plots are shown with $\mu = 0 \text{ MeV}$ and $\mu = T$, respectively.

In figure 3.5(a) one can see, that the chiral condensate is constant in ϕ at zero temperature. Not surprisingly, the chiral condensate is asymptotically increasing in T for all mass parameters and $\mu = 0 \text{ MeV}$ around $\phi = 0$ (bosonic range), while it converges asymptotically to zero if ϕ is not close to zero (fermionic range). The chiral condensate approaches zero continuously, so that, speaking in words of thermodynamics, only a cross-over occurs. In case of $\mu = T$, $\langle \bar{\psi}\psi \rangle_{\phi}$ vanishes for arbitrary boundary conditions with increasing temperature, which is the expected behavior, since the bosonic chiral condensate vanishes alongside $\mu = T$, too. In this case the

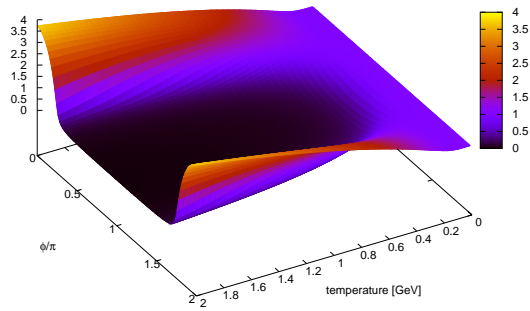


(a) $\mu = 0$ MeV

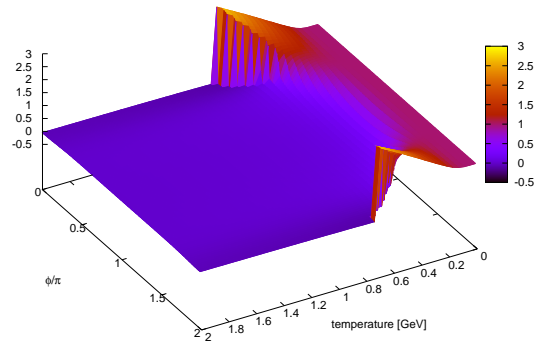


(b) $\mu = T$

Figure 3.6.: ϕ -dependent chiral condensate in the chiral limit, normalized to its value at $T = 0$ MeV

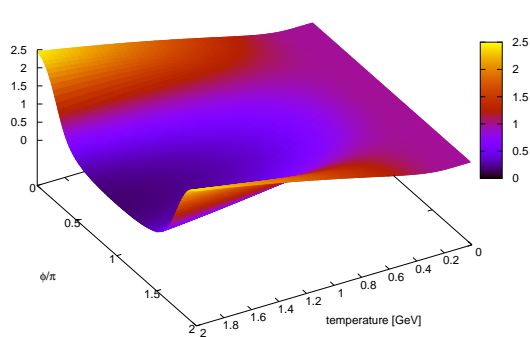


(a) $\mu = 0$ MeV

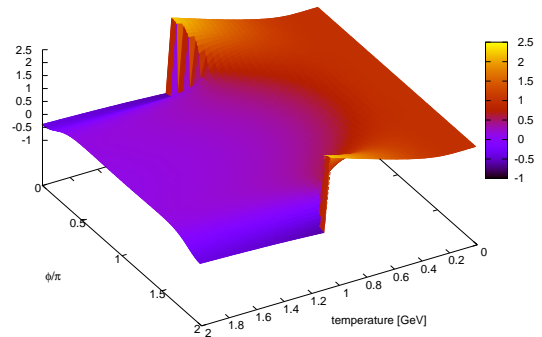


(b) $\mu = T$

Figure 3.7.: ϕ -dependent chiral condensate for $m = 55$ MeV, normalized to its value at $T = 0$ MeV



(a) $\mu = 0$ MeV



(b) $\mu = T$

Figure 3.8.: ϕ -dependent chiral condensate for $m = 550$ MeV, normalized to its value at $T = 0$ MeV

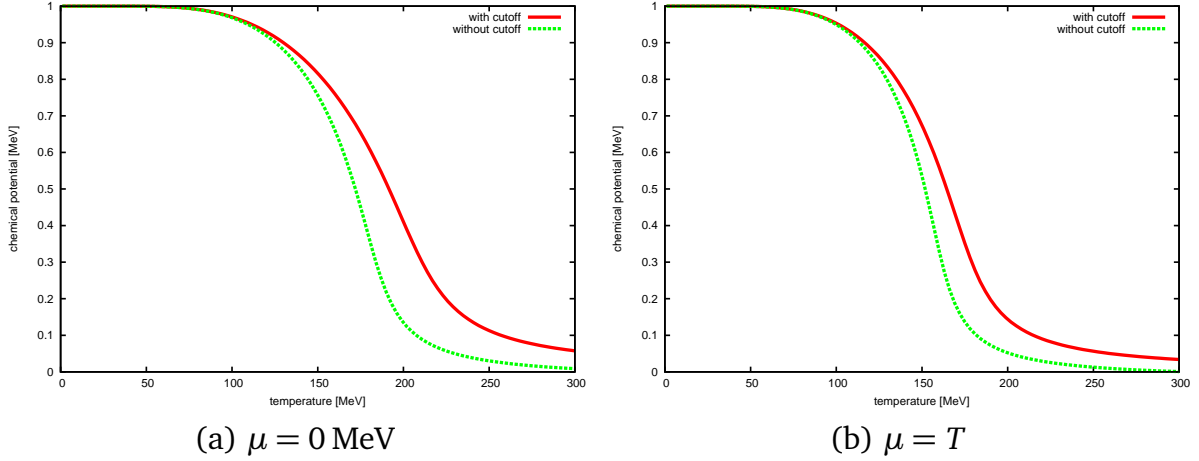


Figure 3.9.: Fermionic chiral condensate with and without cutoff for the thermal part. The chemical potential is zero on the left hand side and equals the temperature on the right hand side. The conventional bare quark mass has been used and the value at $T = \mu = 0$ MeV has been applied as a scale factor.

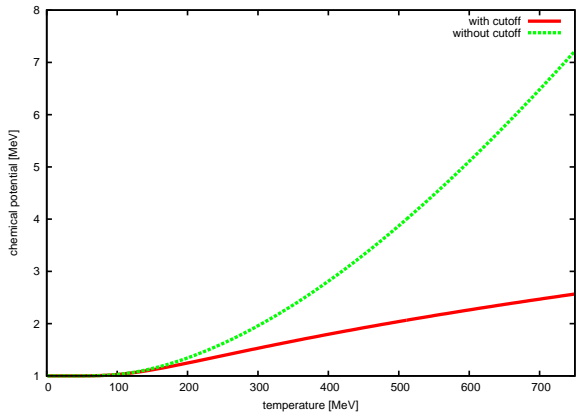
changeover in the bosonic range is a sharp edge and therefore reminds of a first-order phase transition.

Besides the displacement of the cross-over, the T - ϕ -diagrams at larger bare quark masses show the same behavior. In the chiral limit the ($\mu=T$)-diagram shows the same first order transition in the bosonic range, while the transition in the fermionic range and in case of zero chemical potential is of second order. Naturally, the transition in the fermionic range is of first order for all bare quark masses, if $\frac{\mu}{T}$ is big enough to cause a first-order phase transition in the fermionic T - μ -phase diagram.

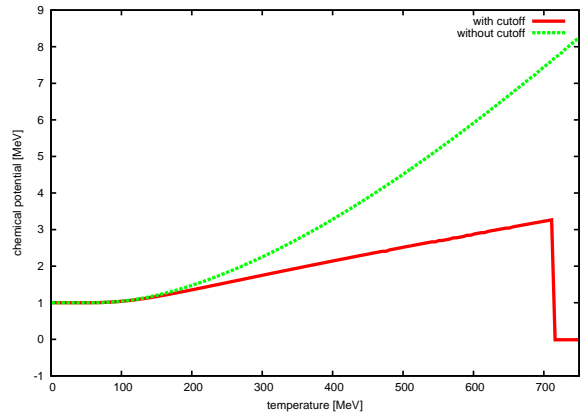
3.4 Chiral Condensate without Thermal Cutoff

All previous plots have been generated using a cutoff in the thermal integral of equations (2.20) and (2.24). As mentioned before, this cutoff is not necessarily applied and can be omitted yielding slightly different results.

The fermionic chiral condensate is plotted with and without thermal cutoff in figure 3.9. Overall, the fermionic chiral condensate is barely sensitive to the cutoff, only the location of the cross-over has changed a little. On the contrary, the bosonic chiral condensate (shown in figure 3.10) shows a crucial difference when using a cutoff in the thermal integral: In case of zero quark chemical potential the bosonic chiral condensate is proportional to the temperature when the cutoff is applied, while it seems to be increasing at least quadratically, if the cutoff is omitted. If $\mu = T$ the difference becomes even more evident. Without any cutoff the bosonic quark condensate grows like in case of zero chemical potential, whereas the condensate with cutoff instantaneous drops to a value near zero at $T \approx 700$ MeV, suggesting a first-order phase transition.

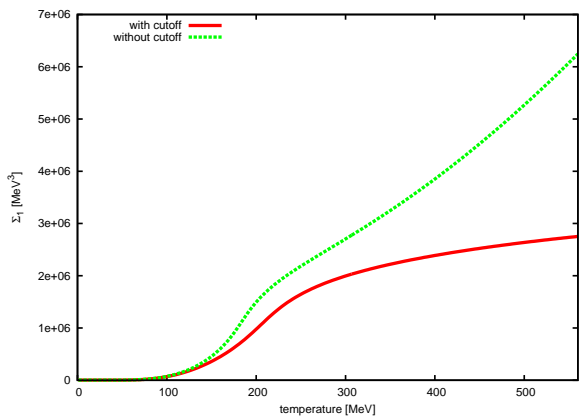


(a) $\mu = 0$ MeV

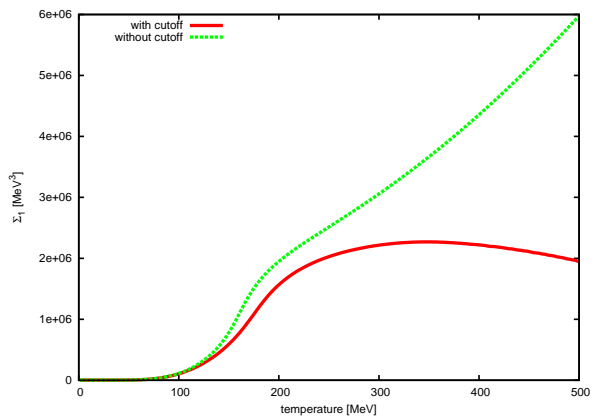


(b) $\mu = T$

Figure 3.10.: Bosonic chiral condensate like the fermionic one in figure 3.9.



(a) $\mu = 0$ MeV



(b) $\mu = T$

Figure 3.11.: Dressed Polyakov loop with and without cutoff for the thermal part for $m = 5.5$ MeV. The chemical potential is zero on the left hand side and equals the temperature on the right hand side.

3.5 Consequences on the Dressed Polyakov Loop

The previously discussed behavior has extensive influence on the dressed Polyakov loop, that can be seen in figure 3.11. One can see, that the dressed Polyakov loop seems to be unbounded when no thermal cutoff is applied, regardless of the chemical potential, which is a direct outcome of the behavior of the bosonic quark condensate without thermal cutoff. Using the cutoff in the thermal integral yields different results depending on the choice of μ . In case of $\mu = 0$ MeV the dressed Polyakov loop seems to rise permanently, though not as fast as the dressed Polyakov loop without cutoff; if $\mu = T$ the dressed Polyakov loop reaches a maximum and decreases afterwards.

As seen before, the dressed Polyakov loop is defined as an integral over the ϕ -dependent chiral condensate, which equals zero for high temperature and small quark chemical potential, if a thermal cutoff is applied. Accordingly, the dressed Polyakov loop drops to zero for high temperatures, too (figure 3.11(b)). The only exception is a small chemical potential (figure 3.11(a)), since the chiral condensate is monotonously increasing with respect to the temperature in the bosonic region in this case. Consequently, the dressed Polyakov loop permanently increases with rising temperature, too. Either way, the dressed Polyakov loop does not reach a plateau and can not be normalized using some maximum value like it is done with the fermionic chiral condensate. Hence, if the dressed Polyakov loop serves as an order parameter, one has to consider another criterion than the crossing of some line, in order to check, where the phase transition or cross-over occurs.

Notice, that the dressed Polyakov loop is liable to regularization effects, since it diverges or drops to zero depending on the choice of regularization.

With increasing chemical potential the chiral cross-over occurs at lower temperature independent of the boundary condition (see section 3.3). This ϕ -independent effect causes the dressed Polyakov loop to act that way, that the possible phase transition or cross-over happens to take place at lower temperature for high values of $\frac{\mu}{T}$, which is exactly the behavior of the chiral cross-over.

3.6 The Dressed Polyakov Loop as an Order Parameter

As discussed before (section 3.5), the dressed Polyakov loop is asymptotically divergent in T , for small values of the quark chemical potential, and drops to zero otherwise, which makes it difficult to interpret the dressed Polyakov loop as an order parameter as easily as the chiral condensate. The following plots 3.12 to 3.15 show the fermionic chiral condensate and dressed Polyakov for various values of $\frac{\mu}{T}$ and bare quark masses. The chiral condensate is normalized to equal one at zero temperature and the same scale factor is applied to the dressed Polyakov loop.

One can notice, that the cross-over (chiral phase transition in the chiral limit), indicated by the dressed Polyakov loop seems to occur at the same temperature as the cross-over stated by the chiral condensate. In order to compare the chiral condensate and dressed Polyakov loop, one has to consider how to determine the temperature where the cross-over takes place.

Two possible criteria for the location of the chiral cross-over are the intersection of the normalized chiral condensate with the $\frac{1}{2}$ -line and the inflection point, that is the maximum of the

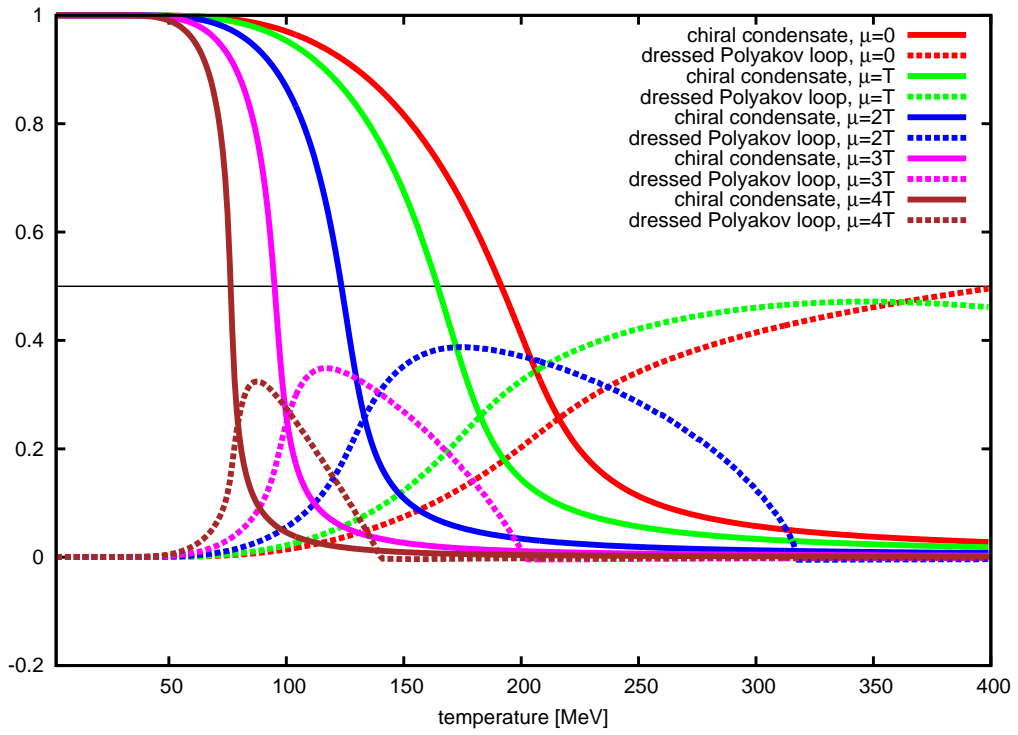


Figure 3.12.: Normalized chiral condensate and dressed Polyakov loop for $m = 5.5$ MeV and various $\frac{\mu}{T}$

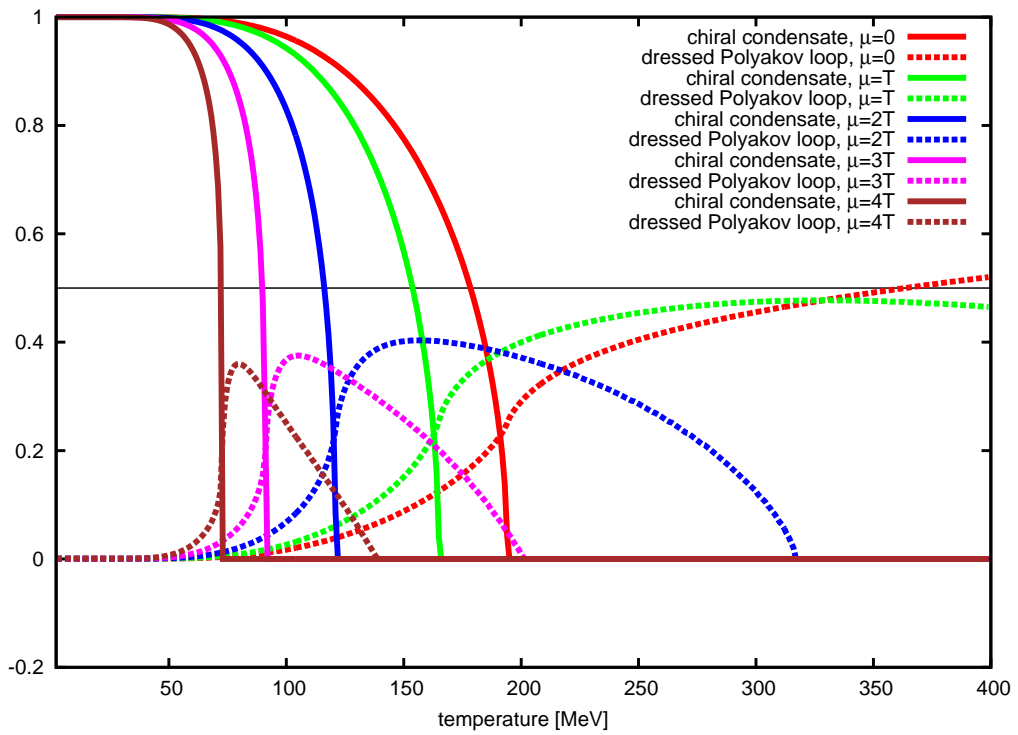


Figure 3.13.: Normalized chiral condensate and dressed Polyakov loop for $m = 0$ MeV and various $\frac{\mu}{T}$

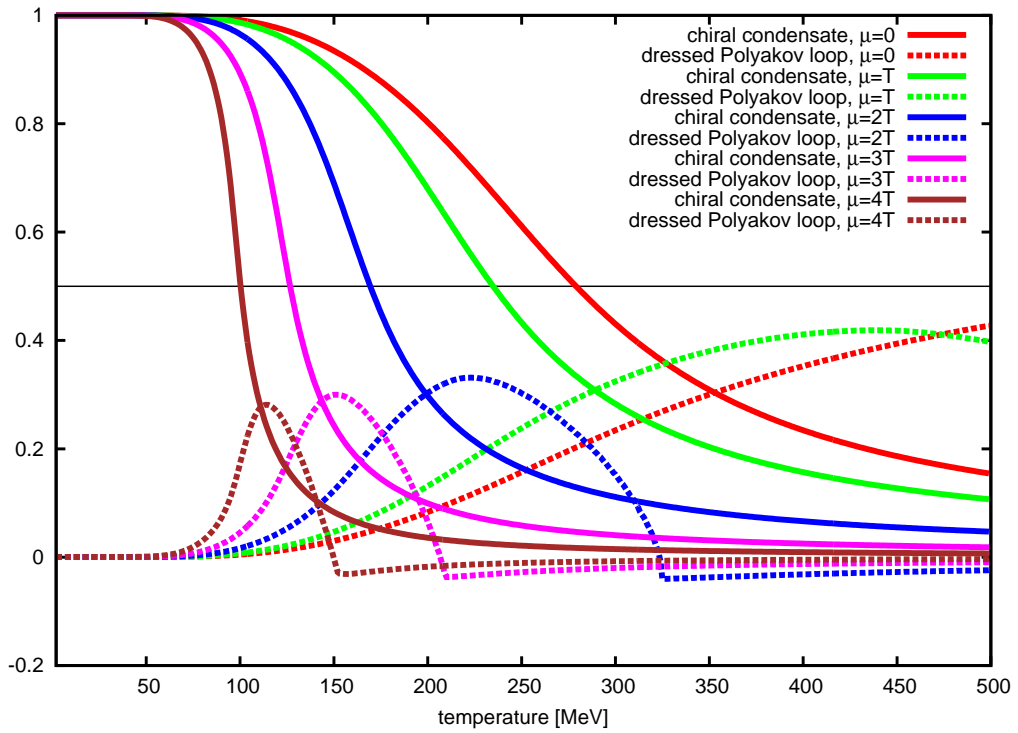


Figure 3.14.: Normalized chiral condensate and dressed Polyakov loop for $m = 55$ MeV and various $\frac{\mu}{T}$

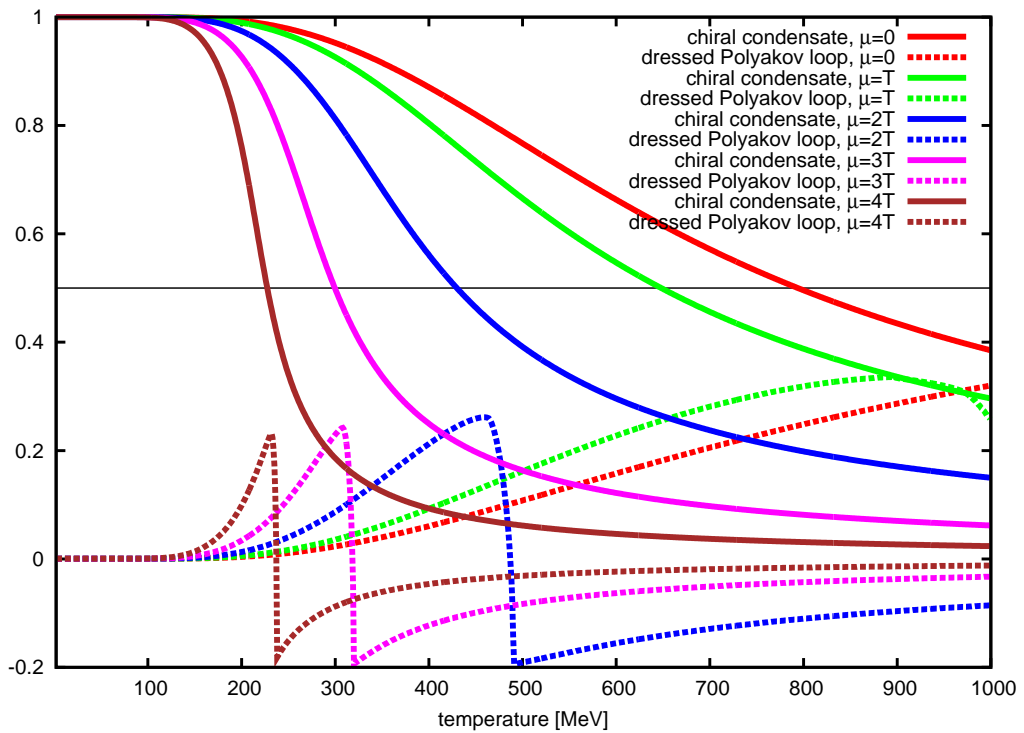
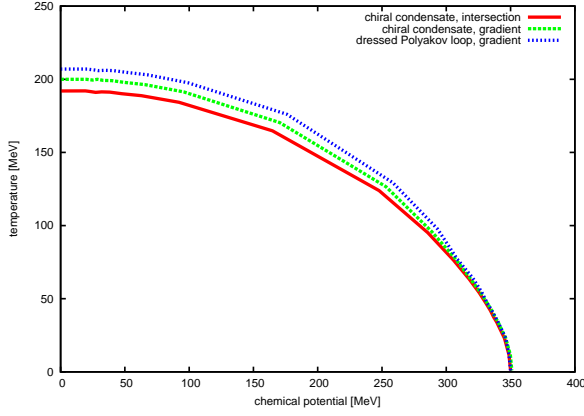
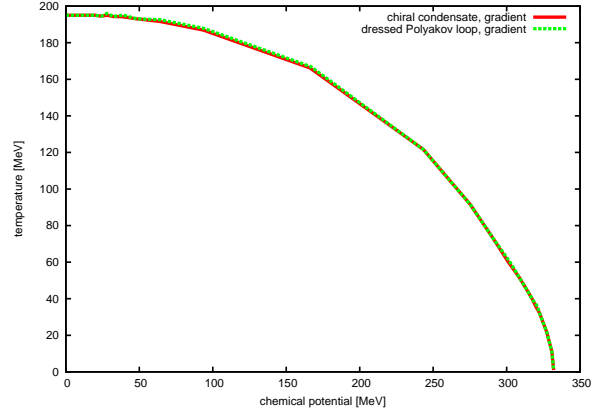


Figure 3.15.: Normalized chiral condensate and dressed Polyakov loop for $m = 550$ MeV and various $\frac{\mu}{T}$

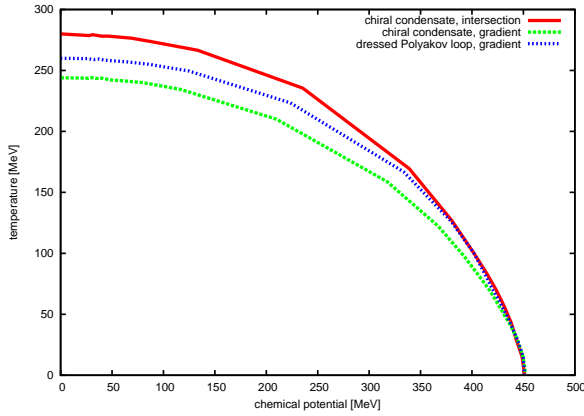


(a) $m = 5.5$ MeV

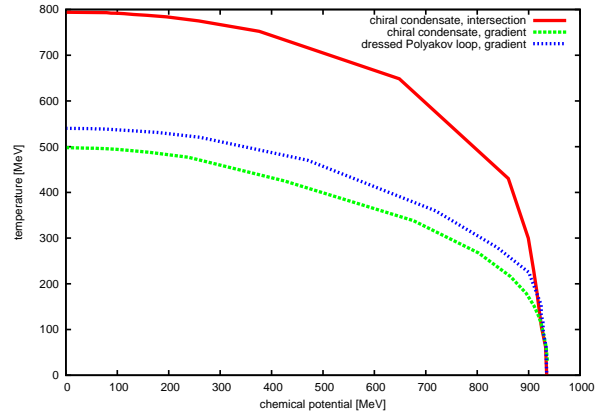


(b) $m = 0$ MeV

Figure 3.16.: μ - T -phase diagrams for conventional bare quark mass (lhs.) and in the chiral limit (rhs.). Note that phase transition in the chiral limit is well-defined, which is why no “intersection”-phase transition is shown.



(a) $m = 55$ MeV



(b) $m = 550$ MeV

Figure 3.17.: μ - T -phase diagrams for tenfold (lhs.) and hundredfold (rhs.) bare quark masses.

first derivative with respect to the temperature. Note that in the chiral limit the phase transition is unambiguously defined to occur, when the chiral condensate vanishes, which is (in this case) identical to the inflection point criterion. The dressed Polyakov loop can not be normalized to its maximum value and thus only its derivative with respect to T can be used to locate the cross-over.

These possibilities sum up to three different phase transitions for each bare quark mass. The following figures 3.16(a) to 3.17(b) show the curves of these phase transitions in the μ - T -diagram.

One can see, that the phase boundary specified by the dressed Polyakov loop completely coincides with the chiral phase boundary. At nonzero bare quark masses the two boundary lines differ and the larger the bare quark masses are, the more disparate they become. Still, the phase boundary lines indicated by the gradient remain close compared to the phase boundary given by the intersection with $\frac{1}{2}$. Especially in figure 3.17(b) the intersection-boundary seems to be mostly unrelated to the other boundary lines. Nevertheless, all three boundary lines are equal below the endpoint, where the first-order phase transition occurs.

3.7 Conclusion

As stated in the beginning, the cross-over of the chiral condensate was expected to become sharper with decreasing bare quark masses resulting in a sharp edge in the chiral limit, corresponding to the chiral phase transition. Furthermore one expected, that the chiral cross-over is blurred in the range of large bare quark masses. These effects can be seen in figures 3.13 and 3.15, respectively. The huge difference between the two chiral boundary lines in figure 3.17(b) confirms the blurred chiral cross-over at large bare quark masses in particular.

In the last chapter we have seen, that the dressed Polyakov loop correctly ascertained every phase transition indicated by the quark condensate. Especially, in the chiral limit, the dressed Polyakov loop serves as an exact order parameter for chiral symmetry breaking. However, the expectation of a sharp edge in the dressed Polyakov loop at large bare quark masses ($m = 550 \text{ MeV}$) is at least fulfilled at $\mu \geq 2T$ (see figure 3.15).

Like in quantum chromodynamics, the cross-over indicated by the quark condensate and dressed Polyakov loop respectively are close-by, even though the NJL model does not include any confinement and hence the dressed Polyakov loop can not specify a confinement-deconfinement cross-over or phase transition.

4 Summary and Outlook

In the beginning we introduced the Lagrangian of a two-flavor NJL model that has a $SU(2) \times SU(2)$ symmetry (chiral symmetry) and a $U(1)$ symmetry in common with the Lagrange density of quantum chromodynamics. We derived the grand canonical potential in mean field approximation, in order to calculate the effective mass and the chiral quark condensate.

Afterwards, the fermionic fields ψ have been generalized to obey arbitrary boundary conditions, which led to a grand potential depending on these boundary conditions. The effective mass and chiral condensate can be defined via derivatives of the grand potential and therefore depend on the boundary conditions, too.

Using the generalized quark condensate, we defined the dressed Polyakov loop, that is an order parameter for confinement in quantum chromodynamics. We discussed the behavior of the ϕ -dependent chiral condensate and investigated its influence on the dressed Polyakov loop.

In a last step, the cross-over boundary of the dressed Polyakov loop and the chiral condensate have been calculated and compared for various bare quark masses. We have seen, that the cross-over temperature of the dressed Polyakov loop and quark condensate coincide, like in quantum chromodynamics, although the NJL model lacks confinement and one has to consider a different interpretation for the dressed Polyakov loop.

The extension to arbitrary boundary conditions has been done with strong approximations. We considered only the real part of the grand canonical potential and the effective mass and the quark condensate were assumed to be real in general. A matter of interest is, whether the results of this work stay correct, when omitting these approximations. So the next step could be to do calculations in a fully complex NJL model.

Alternatively, one could calculate the dressed Polyakov loop and the chiral condensate in the PNJL model (Polyakov–Nambu–Jona-Lasinio model), that is an extension of the NJL model and includes a gluonic part. It is possible to define the thin Polyakov loop in the PNJL model and therefore compare the dressed Polyakov loop and the chiral condensate to a quantity, that specifies confinement cross-over.

A Motivation for the Matsubara Replacement in Thermal Field Theory

Thermal field theory (also named finite temperature field theory) is a combination of conventional quantum field theory and statistical (quantum-)mechanics. As in statistical mechanics, the statistical observables of a quantum field-theoretical system are entirely determined by a partition function. In this work the temperature and chemical potential are fixed, so that the grand canonical partition function is suitable to describe the quantum field-theoretical systems. The grand canonical partition function \mathcal{Z} can be written as

$$\mathcal{Z} = \text{Tr} \{ \hat{\rho} \} \quad (\text{A.1})$$

$$\hat{\rho} = e^{-\beta(\hat{H} - \mu\hat{N})}, \quad (\text{A.2})$$

where $\hat{\rho}$ denotes the density matrix, \hat{H} the Hamiltonian and \hat{N} a particle number operator. Using the basis $|\phi_a\rangle$ fulfilling the completeness relation $\int d\phi_a |\phi_a\rangle \langle\phi_a| = \mathbb{I}$, one can write the trace explicitly as

$$\mathcal{Z} = \text{Tr} \{ e^{-\beta(\hat{H} - \mu\hat{N})} \} = \int d\phi_a \langle\phi_a| e^{-\beta(\hat{H} - \mu\hat{N})} |\phi_a\rangle. \quad (\text{A.3})$$

Now inspect the transition amplitude between a state $|\phi_a\rangle$ and its time evolution using the path integral formalism and the Hamilton density \mathcal{H} :

$$\langle\phi_a| e^{iHt} |\phi_a\rangle = \int \mathcal{D}\pi \int \mathcal{D}\phi \exp \left\{ i \int_0^t dt \int d^3x (\pi\dot{\phi} - \mathcal{H}(\pi, \phi)) \right\} \quad (\text{A.4})$$

Keeping in mind, that a conserved charge forces the replacement

$$\mathcal{H}(\pi, \phi) \rightarrow \mathcal{H}(\pi, \phi) - \mu\mathcal{N}(\pi, \phi), \quad (\text{A.5})$$

the comparison between equation (A.3) and (A.4) suggests, that the grand partition function can be written as functional integral using the transition $\frac{1}{T} = \beta \rightarrow it$.

The expectation value of an operator is defined as $\langle \hat{O} \rangle = \frac{1}{\mathcal{Z}} \text{Tr} \{ \hat{\rho} \hat{O} \}$, so that the propagator of a field can be written as

$$D(x, y) = D(\vec{x}, \vec{y}; x^0, y^0) = \text{Tr} \{ \hat{\rho} T[\phi(x)\phi(y)] \} \quad (\text{A.6})$$

Using the Heisenberg time evolution $\phi(\vec{x}, x^0 + \beta) = e^{\beta\hat{H}} \phi(\vec{x}, x^0) e^{-\beta\hat{H}}$ in Euclidean space, one can show, that the propagator is (anti-)periodic:

$$D(\vec{x}, \vec{y}; x^0, y^0) = \pm D(\vec{x}, \vec{y}; x^0, y^0 + \beta) \quad (\text{A.7})$$

The \pm -sign occurs due to the different definitions of the bosonic and fermionic time ordered products. Furthermore, equation (A.7) implies the periodicity of bosonic and fermionic fields ϕ and ψ respectively.

$$\phi(\vec{x}, x^0) = +\phi(\vec{x}, x^0 + \beta) \quad (\text{A.8})$$

$$\psi(\vec{x}, x^0) = -\psi(\vec{x}, x^0 + \beta) \quad (\text{A.9})$$

This periodicity allows a Fourier series expansion from which the replacement $\int \rightarrow \sum$ arises.

Bibliography

- [1] Y. Nambu and G. Jona-Lasinio, “Dynamical Model of Elementary Particles Based on an Analogy with Superconductivity. I,” *Phys. Rev.*, vol. 122, p. 345, Apr 1961.
- [2] Y. Nambu and G. Jona-Lasinio, “Dynamical Model of Elementary Particles Based on an Analogy with Superconductivity. II,” *Phys. Rev.*, vol. 124, p. 246, Oct 1961.
- [3] J. I. Kapusta, *Finite-Temperature Field Theory*. Cambridge University Press, March 1994.
- [4] M. . Lombardo, “Finite temperature field theory,” *ArXiv High Energy Physics - Phenomenology e-prints*, Mar. 2001. arXiv:hep-ph/0103141v2.
- [5] D. Scheffler, *NJL model study of the QCD phase diagram using the Taylor series expansion technique*. Bachelor thesis, Technische Universität Darmstadt, 2007.
- [6] M. Buballa, “NJL-model analysis of dense quark matter,” *Physics Reports*, vol. 407, p. 205, 2005.
- [7] T. K. Mukherjee, H. Chen, and M. Huang, “Chiral condensate and dressed Polyakov loop in the Nambu–Jona-Lasinio model,” *Phys.Rev.*, vol. D82, p. 034015, 2010.
- [8] E. Bilgici, *Signatures of confinement and chiral symmetry breaking in spectral quantities of lattice Dirac operators*. PhD thesis, Karl-Franzens-Universität Graz.
- [9] A. Knetsch, *The NJL model and the dressed Polyakov Loop*. Bachelor thesis, Technische Universität Darmstadt, 2011.